JACC: CARDIOVASCULAR IMAGING VOL. 7, NO. 2, 2014

ISSN 1936-878X/$36.00
PUBLISHED BY ELSEVIER INC. http://dx.doi.org/10.1016/j.jcmg.2013.09.019

CMR Imaging With Rapid Visual T1 Assessment Predicts Mortality in Patients Suspected of Cardiac Amyloidosis

James A. White, MD,*†‡ Han W. Kim, MD,§‖ Dipan Shah, MD,# Nowell Fine, MD,* Ki-Young Kim, MD,§ David C. Wendell, PHD,§ Wael Al-Jaroudi, MD,§ Michele Parker, MS,§‖ Manesh Patel, MD,‖ Femida Gwadry-Sridhar, PHD,‡ Robert M. Judd, PHD,§‖¶ Raymond J. Kim, MD§‖¶

London, Ontario, Canada; Durham, North Carolina; and Houston, Texas

OBJECTIVES This study tested the diagnostic and prognostic utility of a rapid, visual T1 assessment method for identification of cardiac amyloidosis (CA) in a "real-life" referral population undergoing cardiac magnetic resonance for suspected CA.

BACKGROUND In patients with confirmed CA, delayed-enhancement cardiac magnetic resonance (DE-CMR) frequently shows a diffuse, global hyperenhancement (HE) pattern. However, imaging is often technically challenging, and the prognostic significance of diffuse HE is unclear.

METHODS Ninety consecutive patients referred for suspected CA and 64 hypertensive patients with left ventricular hypertrophy (LVH) were prospectively enrolled and underwent a modified DE-CMR protocol. After gadolinium administration a method for rapid, visual T1 assessment was used to identify the presence of diffuse HE during the scan, allowing immediate optimization of settings for the conventional DE-CMR that followed. The primary endpoint was all-cause mortality.

RESULTS Among patients with suspected CA, 66% (59 of 90) demonstrated HE, with 81% (48 of 59) of these meeting pre-specified visual T1 assessment criteria for diffuse HE. Among hypertensive LVH patients, 6% (4 of 64) had HE, with none having diffuse HE. During 29 months of follow-up (interquartile range: 12 to 44 months), there were 50 (56%) deaths in patients with suspected CA and 4 (6%) in patients with hypertensive LVH. Multivariable analysis demonstrated that the presence of diffuse HE was the most important predictor of death in the group with suspected CA (hazard ratio: 5.5, 95% confidence interval: 2.7 to 11.0; $p < 0.0001$) and in the population as a whole (hazard ratio: 6.0, 95% confidence interval 3.0 to 12.1; $p < 0.0001$). Among 25 patients with myocardial histology obtained during follow-up, the sensitivity, specificity, and accuracy of diffuse HE in the diagnosis of CA were 93%, 70%, and 84%, respectively.

CONCLUSIONS Among patients suspected of CA, the presence of diffuse HE by visual T1 assessment accurately identifies patients with histologically-proven CA and is a strong predictor of mortality. (J Am Coll Cardiol Img 2014;7:143–56) © 2014 by the American College of Cardiology Foundation

From the *London Health Sciences Center, Division of Cardiology, University of Western Ontario, London, Ontario, Canada; †Robarts Research Institute, University of Western Ontario, London, Ontario, Canada; ‡Lawson Health Research Institute, University of Western Ontario, London, Ontario, Canada; §Duke Cardiovascular Magnetic Resonance Center, Duke University Medical Center, Durham, North Carolina; ‖Division of Cardiology, Duke University Medical Center, Durham, North Carolina; ¶Department of Radiology, Duke University Medical Center, Durham, North Carolina; and #The Methodist DeBakey Heart Center, Houston, Texas. Funding for the research was provided in part by National Institutes of Health grant RO1-HL64726 (Dr. R. Kim). Dr. White is a clinician scientist with the Heart and Stroke Foundation of Ontario, Canada. Dr. Patel has received research grants from Johnson and Johnson, AstraZeneca, the National Heart, Lung and Blood Institute, and the Agency for Healthcare Research and Quality; and has served on the advisory board for Genzyme and Jansen. Drs. Judd and R. Kim are

The diagnosis of cardiac amyloidosis (CA) should be considered in patients with systemic amyloidosis and those with unexplained left ventricular hypertrophy (LVH) or diastolic heart failure. As CA portends poor prognosis (1), its confirmation or exclusion becomes critical for therapeutic decision-making and patient counseling. Although consensus guidelines indicate that invasive endomyocardial biopsy (EMB) is reasonable in patients with unexplained restrictive cardiomyopathy and suspicion of CA, there are procedural risks and there is uncertainty about sampling error (2). Echocardiography is the most commonly used imaging test in the diagnostic workup, but characteristic findings such as ventricular hypertrophy and restrictive filling pattern are not specific for CA and may be insensitive for early disease (3,4).

See page 166

ABBREVIATIONS AND ACRONYMS

CA = cardiac amyloidosis
CAD = coronary artery disease
CMR = cardiac magnetic resonance
DE-CMR = delayed-enhancement cardiac magnetic resonance
ECG = electrocardiogram
EMB = endomyocardial biopsy
HE = hyperenhancement
IQR = interquartile range
LV = left ventricular
LVH = left ventricular hypertrophy

Recently, several studies have suggested that delayed-enhancement cardiac magnetic resonance (DE-CMR) represents a promising technique for the diagnosis of CA (4–9). These investigations report the high prevalence of a diffuse, global subendocardial hyperenhancement (HE) pattern on DE-CMR in patients with confirmed CA. This pattern is distinctive and appears specific to CA, but the diffuse nature of HE presents challenges for conventional DE-CMR, as a normal reference myocardium—used to provide context for setting pulse sequence parameters and for visual interpretation—may be absent. Perhaps in part due to the imaging challenges, the 3 studies to date that have investigated the prognostic role of DE-CMR in patients with CA have yielded inconsistent results (4,8,10); however, the studies were small and had few events.

The purpose of the current study was to evaluate the diagnostic and prognostic utility of a rapid, visual T1 assessment method for identification of CA. In this investigation, we enrolled consecutive patients referred to cardiac magnetic resonance (CMR) with suspected (but not known) CA to prospectively test the practical clinical value of our new approach in a "real-life" population encountered during the routine practice of CMR.

METHODS

Patient population. STUDY DESIGN. This was a prospective cohort study that enrolled patients consecutively referred to the Duke Cardiovascular Magnetic Resonance Center between March 2003 and July 2007. A total of 154 patients were enrolled: 90 with suspected CA and 64 with hypertensive LVH. Eleven patients with suspected CA were also recruited at Nashville Heart Cardiovascular MRI Center for a pilot phase used to optimize the imaging protocol, and 8 normal subjects without history of cardiac disease were recruited at Duke for quantitative T1 measurements. All patients signed informed consent prior to enrollment, and each institution's research ethics board approved the study.

ENROLLMENT. Similar to previous studies (4,7), patients referred to CMR for suspected CA had at least 1 of the following: pathology-confirmed systemic amyloidosis (extracardiac tissue biopsy); confirmed plasma cell dyscrasia; or echocardiographic and/or invasive hemodynamic evidence of a restrictive cardiomyopathy. Patients with known CA by EMB at the time of enrollment were excluded. Hypertensive patients with LVH were recruited during the same enrollment period; they were required to have a diastolic wall thickness ≥12 mm of either the anteroseptal or posterior wall on cine-CMR and were excluded for any documented clinical history of coronary artery disease (CAD) or cardiomyopathy. Hypertensive patients with a history of chest discomfort required a normal stress test or x-ray coronary angiogram (no lesion ≥50% of lumen) before enrollment. Some patients were enrolled before the Food and Drug Administration alerts regarding the rare occurrence of nephrogenic systemic fibrosis associated with gadolinium contrast administration (11). None of the study participants developed nephrogenic systemic fibrosis during the course of the study.

Cardiac magnetic resonance. IMAGING PROTOCOL. CMR was performed on 1.5-T scanners (Sonata or Avanto, Siemens, Erlangen, Germany) using phased-array receiver coils. Cine images were acquired in multiple short-axis (every 10 mm throughout the entire left ventricle) and 3 long-axis views using a steady-state free-precession sequence (slice thickness 6 mm; interslice gap 4 mm; repetition time (TR)

inventors of a U.S. patent on Delayed Enhancement CMR, which is owned by Northwestern University. All other authors have reported that they have no relationships relevant to the contents of this paper to disclose.

Manuscript received September 26, 2013; accepted September 27, 2013.

3.0 ms; echo time (TE) 1.5 ms; temporal resolution 35 to 40 ms; flip angle 60°; and in-plane resolution ~1.7 × 1.4 mm).

Delayed-enhancement imaging was performed in 2 distinct ways after gadolinium contrast administration (gadoversetamide, 0.15 mmol/kg). First, T1 assessment was performed 5 to 10 min after contrast using a breath-hold, inversion-recovery cine-SSFP pulse sequence (5,12,13), in which sequential phases of the cardiac cycle were acquired at increasing time from the inversion pulse in 30 ms increments (starting at 80 ms). Midventricular short-axis and 4-chamber long-axis views were obtained, and T1 assessment was usually completed in 1 to 2 min (i.e., 2 breath-holds). Other imaging parameters were: slice thickness 8 mm; TR 2.2 ms; TE 1.1 ms; flip angle 50°; in-plane resolution ~2.5 × 1.7 mm; and repetition time between inversion pulses: 2 R-R intervals.

The purpose of T1 assessment was to provide an objective method for the identification of diffuse HE. Following completion of the first pass of gadolinium, normal myocardium will have a considerably lower concentration of contrast than blood and, therefore, should have a far longer T1. A shorter (or similar) T1 would indicate abnormal myocardium with increased gadolinium retention. To exploit this relationship, we performed a frame-by-frame visual comparison of myocardial and blood pool signal over the range of increasing inversion times to determine relative T1s (Fig. 1). If myocardial tissue crossed the null point (i.e., became black) at an earlier or at the same inversion time as blood, the T1 of that tissue was considered abnormally short. Similar to that described previously (7), if >50% of the left ventricular (LV) myocardium on either the short- or long-axis images had abnormally short T1 in an area that was not in a typical coronary artery distribution, then diffuse HE was considered present.

Conventional DE-CMR was then performed using a segmented inversion-recovery gradient-echo sequence (slice thickness 6 mm; interslice gap 4 mm; TR 9.5 ms; TE 3.8 ms; flip angle 25°; in-plane resolution 1.8 × 1.4 mm) in the identical locations as cine-CMR (14,15). However, the inversion delay time was set in a specific manner. In patients meeting criteria for diffuse HE, the inversion time prescribed was that which best demonstrated the extent of abnormal tissue enhancement by T1

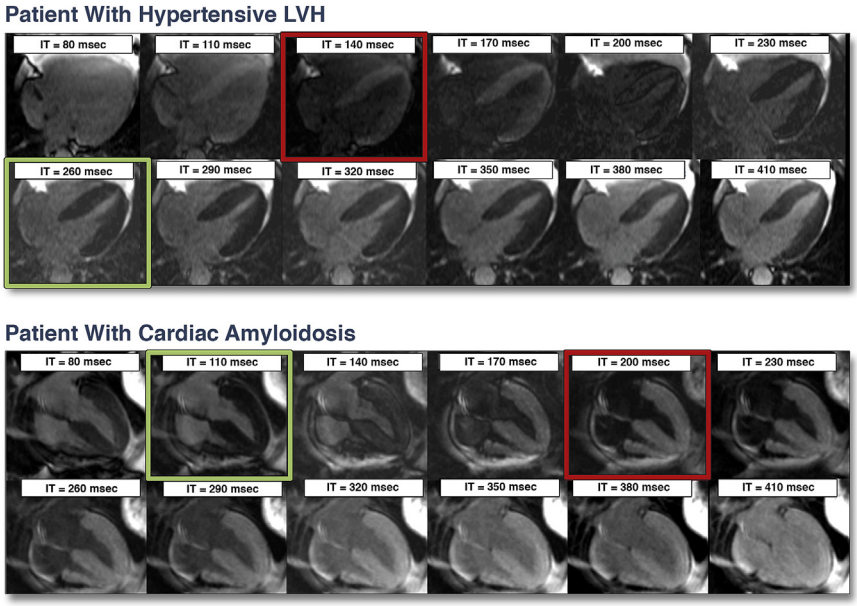

Figure 1. Examples of T1 Assessment in a Patient With Hypertensive LVH and in a Patient With Suspected Cardiac Amyloidosis Later Confirmed by Biopsy

Each set of images was acquired in a single breath-hold 5 min after gadolinium administration. The time from the inversion pulse (IT) is shown in each frame. In the patient with left ventricular hypertrophy (LVH) **(top)**, the blood pool reaches the null point (becomes black, **red square**) before—that is, at an earlier IT than—the myocardium **(green square)**. This is the normal relationship in patients without hyperenhancement, and indicates that after contrast, the T1 of normal myocardium is longer than that of blood. Conversely, in the patient with cardiac amyloidosis **(bottom)**, the entire myocardium crosses the null point prior to the blood pool, indicating the presence of diffuse, global hyperenhancement. Note that, in isolation, the image with myocardium "nulled" **(green square)** appears to show that all myocardium is normal, demonstrating the pitfalls of conventional DE-CMR without T1 assessment.

assessment. This was the inversion time required to either null the blood pool (if no normal myocardium was present) or, if present, normal myocardium. In patients not demonstrating diffuse HE, the inversion time was prescribed in the conventional fashion with an aim to null normal myocardium (15).

IMAGE ANALYSIS. Cine and DE-CMR images were evaluated separately, masked to all patient information. Quantitative measurements of LV wall thickness, mass, volumes, and ejection fraction were obtained from the stack of short-axis cine images using standard methods (14). The presence of pericardial and pleural effusions on cine-CMR was scored in a binary fashion, with trace effusions being considered normal. DE-CMR images were interpreted by consensus of 2 experienced readers (J.A.W. and H.W.K.); a pre-designated third reader (R.J.K.) was consulted in cases of interpretive discordance. The presence of diffuse HE was determined from T1 assessment as described earlier (Fig. 1). This was followed by inspection of conventional DE-CMR images for other (focal) patterns of HE, and these were scored either as CAD type when they were subendocardial or transmural in a typical vascular distribution, or as non-CAD type when they were midmyocardial or epicardial (16). Intraobserver and interobserver variability of visual T1 assessment was tested in 20 patients, 10 of whom were randomly chosen from the subgroup with diffuse HE and 10 from the subgroup without diffuse HE. Images were interpreted several months after the initial read. For both intraobserver and interobserver testing, there was 100% agreement with the initial read in separating patients with and without diffuse HE.

Electrocardiography. Twelve-lead electrocardiograms (ECGs), obtained a median of 1 day after CMR (interquartile range [IQR]: 0 to 3 days), were available in 133 patients overall: 80 (89%) with suspected CA and 53 (83%) with hypertensive LVH. These were masked to patient identity and interpreted for low ECG voltage as described by Rahman et al. (17) (total height of the QRS complex <5 mm in the limb leads and <10 mm in the precordial leads), and were assessed for the presence of Q waves using Minnesota codes 1-1-1 through 1-2-7 [18]).

Echocardiography. Transthoracic echocardiograms, obtained a median of 1 day prior to CMR (IQR: 4 days before to 2 days after), were available in 99 patients overall: 64 (71%) with suspected CA and 35 (55%) with hypertensive LVH. These were digitally copied, masked for blinded review, and analyzed on a commercial workstation (Xcelera, Philips Medical Systems, Best, the Netherlands). The following were measured as previously described (19): LV wall thickness (mean of anteroseptal and posterior walls), peak early to late diastolic velocity (E/A) ratio, mitral inflow deceleration time (DT), and mitral annular septal velocity (E′). All measurements were made over 3 cardiac cycles and averaged. Abnormal diastolic function was classified according to standard criteria into 3 dysfunctional filling patterns: slow relaxation, pseudonormal, or restrictive (19).

Clinical follow-up. Clinical information related to the occurrence of adverse events was obtained via: 1) telephone interview with the patient or, if deceased, family members; 2) contact with the patient's physician(s); 3) hospital records; and 4) death certificates. The pre-specified primary endpoint was all-cause mortality. The secondary endpoint was a composite of death, cardiac transplantation, or hospital admission for heart failure. The latter required administration of intravenous diuretics for the treatment of pulmonary edema (confirmed by clinical examination and chest x-ray) or peripheral edema. For the primary endpoint, all-cause rather than cardiac mortality was used because the former is objective, clinically relevant, and unbiased, which is often not the case for cardiac mortality (20). Cardiac troponin T levels, if measured, were also recorded.

Myocardial histopathology. All cardiac tissue obtained during the follow-up period from endomyocardial biopsy, cardiac transplantation, or autopsy were evaluated in a systematic manner. Samples were examined by light microscopy, immunofluorescence, and electron microscopy. Amyloid protein was considered present upon demonstration of apple-green birefringence under polarized light or the appearance of amyloid fibrils on electron microscopy (21). Immunohistochemical stains using commercially-available antisera to kappa and lambda immunoglobulin light chains were also employed (21,22).

Statistical analysis. Continuous data were expressed as mean ± SD, or in cases in which the distribution was not normal, as median and interquartile range. Comparisons of continuous data between groups were made using 2-sample t test or the Wilcoxon rank sum test as appropriate. The chi-square test was used to make between-group comparisons of discrete data. To identify variables associated with adverse outcome, univariable Cox proportional hazards regression analysis was performed. Multivariable models were subsequently developed using 2 approaches. In the first, candidate variables showing a possible association with prognosis by univariable analysis ($p < 0.05$) were

considered 1 at a time starting with the most significant candidate. Final model variables were determined by stepwise selection (and backwards elimination) at the level of significance of $p = 0.05$. In the second approach, only 4 variables were included to avoid the potential for overfitting. These were 3 well-known clinical markers of prognosis in cardiac amyloidosis—LV ejection fraction, ECG low-voltage pattern, and LV mass (23)—and HE. For both approaches, 2 submodels were constructed, 1 including "diffuse" HE and the other including "any" HE. Results were presented as hazard ratios (HRs) and their associated 95% confidence intervals (CIs) for the model variables, as well as likelihood ratios for the models. Cumulative event rates were calculated according to the Kaplan-Meier method. Comparisons between survival curves were made using Cox regression analysis after adjusting for other significant covariates from the multivariable models. All statistical tests were 2-tailed, and $p < 0.05$ was regarded as significant. S-Plus (version 8.0, Insightful Software, Seattle, Washington) was used to perform the statistical analyses.

RESULTS

Patient characteristics. Among patients with suspected CA, 46 (51%) had documented systemic (extracardiac) amyloidosis at the time of enrollment: 41 had monoclonal light chain amyloid, 2 had secondary amyloid, and 3 had hereditary amyloid (2 with variant transthyretin, 1 with variant fibrinogen). Of the remaining 44 patients with suspected CA, 16 had a diagnosis of plasma cell dyscrasia and 28 had echocardiographic and/or invasive hemodynamic evidence of restrictive cardiomyopathy.

Baseline characteristics are shown in Table 1 for patients with suspected CA in comparison with those with hypertensive LVH. Patients with suspected CA were slightly older, had worse New York Heart Association (NYHA) functional class, more often had signs of right heart failure (peripheral edema and/or ascites in the presence of an elevated jugular venous pressure), and were more likely to have low voltage on ECG. Patients with suspected CA also had higher E/A ratios, had shorter deceleration times, and were more likely to have pseudonormal or restrictive diastology on echocardiography. On cine-CMR, there were no significant differences in LV mass index or LV end-diastolic volume index, but there was a mild increase in LV end-systolic volume index, leading to a comparative decrease in LV ejection fraction (median 56% vs. 69%). There was also a higher prevalence of pericardial (50% vs. 14%) and pleural effusions (48% vs. 9%) in the group with suspected CA.

DE-CMR findings. Figure 2 summarizes the DE-CMR findings in the 2 cohorts. Among patients with suspected CA, 59 (66%) demonstrated HE, 81% (48 of 59) of whom met visual T1 assessment criteria for diffuse HE. Focal CAD-type HE was observed in 11 patients, 6 of whom also had diffuse HE. Focal non–CAD-type (midwall or epicardial) HE was noted in 6 patients, none of whom had diffuse HE concurrently. Among hypertensive LVH patients, 4 (6%) had HE, and none were diffuse. Findings in the subgroup of 46 patients with documented systemic (extracardiac) amyloidosis at the time of enrollment are also shown in Figure 2. A total of 34 patients (74%) had HE, 85% (29 of 34) of whom had diffuse HE. Typical CMR images of patients with diffuse HE are shown in Figure 3.

The mean difference in inversion times corresponding to the frames where blood and myocardial signals were nulled was 50 ± 30 ms (range 0 to +125 ms) for patients with diffuse HE and -72 ± 25 ms (range -110 to -43 ms) for hypertensive LVH patients ($p < 0.0001$). Blood T1 was estimated based on the inversion time (IT) to null blood ($T1 = [1/\ln(2)] \times IT[null]$) and found to be 313 ± 70 ms in patients with diffuse HE and 285 ± 68 ms in hypertensive patients. In 8 normal subjects without history of cardiac disease, T1 assessment was performed until 30 min post-contrast to test if T1 of normal myocardium may become shorter than that of blood within a clinically-relevant time period. In all 8 patients, the T1 of normal myocardium remained longer than that of blood, with a mean difference of 76 ± 30 ms (range 36 to 119 ms) at 30 min.

Survival. ENTIRE POPULATION. The median follow-up time was 29 months (IQR: 12 to 44 months). No patient was lost to follow-up. During this period there were 50 (56%) deaths in patients with suspected CA and 4 (6%) deaths in patients with hypertensive LVH ($p < 0.0001$). The relationships between clinical and CMR characteristics with the primary endpoint of all-cause mortality are shown in Table 2. Among the characteristics that were significantly associated with mortality, "diffuse" and "any" HE were the strongest univariable predictors (highest t statistic). For multivariable analysis, separate submodels were constructed, 1 including "diffuse" HE and the other including "any" HE. Table 2 demonstrates that NYHA functional class, serum creatinine, the presence of pleural effusion,

Table 1. Baseline Patient Characteristics

	Suspected CA (n = 90)	Hypertensive LVH (n = 64)	p Value
Age, yrs	62 ± 13	57 ± 13	**0.01**
Male	52 (58)	46 (72)	0.07
NYHA functional class	3.0 (1.0, 3.0)	1.0 (1.0, 2.0)	**<0.0001**
Right heart failure	54 (60)	5 (8)	**<0.0001**
Dialysis	13 (14)	1 (2)	**0.01**
Systolic blood pressure, mm Hg	120.9 ± 23.4	148.2 ± 26.0	**<0.0001**
Diastolic blood pressure, mm Hg	71.6 ± 11.9	86.4 ± 15.1	**<0.0001**
Serum creatinine, mg/dl	1.2 (1.0, 2.3)	1.1 (1.0, 1.4)	0.06
Electrocardiography*			
Low voltage†	50 (63)	9 (17)	**<0.0001**
Q wave‡	6 (8)	3 (6)	0.68
Echocardiography§			
Mean LV wall thickness, mm	14.2 ± 3.2	14.0 ± 3.2	0.72
E/A ratio	2.1 (1.1, 2.9)	1.0 (0.8, 1.5)	**<0.0001**
Deceleration time, ms	156 (124, 188)	200 (172, 236)	**<0.0001**
Deceleration time <160 ms	35 (55)	6 (17)	**0.0003**
E/E′ ratio	19.4 (14.3, 28.6)	17.8 (10.3, 28.3)	0.39
E/E′ ratio >15	45 (71)	20 (56)	0.17
Pseudonormal or restrictive diastology	41 (65)	11 (31)	**0.002**
Cine-CMR			
Mean LV wall thickness, mm	12.8 ± 3.8	12.5 ± 3.4	0.63
LV mass index, g/m^2	91 (69, 126)	83 (69, 107)	0.21
LV EDV index, ml/m^2	58 (43, 76)	66 (53, 77)	0.09
LV ESV index, ml/m^2	24 (18, 36)	22 (13, 30)	**0.04**
LV ejection fraction, %	56 (47, 65)	69 (61, 73)	**<0.0001**
Pericardial effusion	45 (50)	9 (14)	**<0.0001**
Pleural effusion	43 (48)	6 (9)	**<0.0001**
DE-CMR			
Any HE	59 (66)	4 (6)	**<0.0001**
Diffuse HE	48 (53)	0 (0)	**<0.0001**
CAD-type HE	11 (12)	2 (3)	**0.05**
Focal non-CAD-type HE (midwall or epicardial)	6 (7)	2 (3)	0.47

Values are mean ± SD, n (%), or median (25th, 75th percentile). Numbers in boldface indicate p values ≤0.05. *Available in 133 patients, 80 with suspected CA and 53 with hypertensive LVH; †defined as total height of the QRS complex <5 mm in the limb leads and <10 mm in the precordial leads; ‡defined by Minnesota codes 1-1-1 through 1-2-7; §available in 99 patients, 64 with suspected CA and 35 with hypertensive LVH.
CA = cardiac amyloidosis; CAD = coronary artery disease; CMR = cardiac magnetic resonance; DE = delayed-enhancement; E/A = peak early to late diastolic velocity; EDV = end-diastolic volume; ESV = end-systolic volume; HE = hyperenhancement; LV = left ventricular; LVH = left ventricular hypertrophy; NYHA = New York Heart Association.

and the respective HE variable were independent predictors of mortality in both submodels. For submodel 1, diffuse HE was the strongest predictor (highest *t* statistic), with an HR of 6.0 (95% CI: 3.0 to 12.1; $p < 0.0001$). For submodel 2, any HE was the strongest predictor, with an HR of 6.5 (95% CI: 3.0 to 14.2; $p < 0.0001$). Overall, the 2 submodels had similar predictive capabilities, with chi-square values of 100.2 and 99.7, respectively.

Concerning the secondary endpoint, there were 54 (56%) patients with suspected CA and 8 (13%) with hypertensive LVH who experienced death, cardiac transplantation, or hospital admission for heart failure during follow-up. Results from multivariable analyses were similar to that for the primary endpoint in that diffuse HE was the strongest predictor in submodel 1 (HR: 5.8, 95% CI: 3.2 to 10.5; $p < 0.0001$) and any HE was the strongest

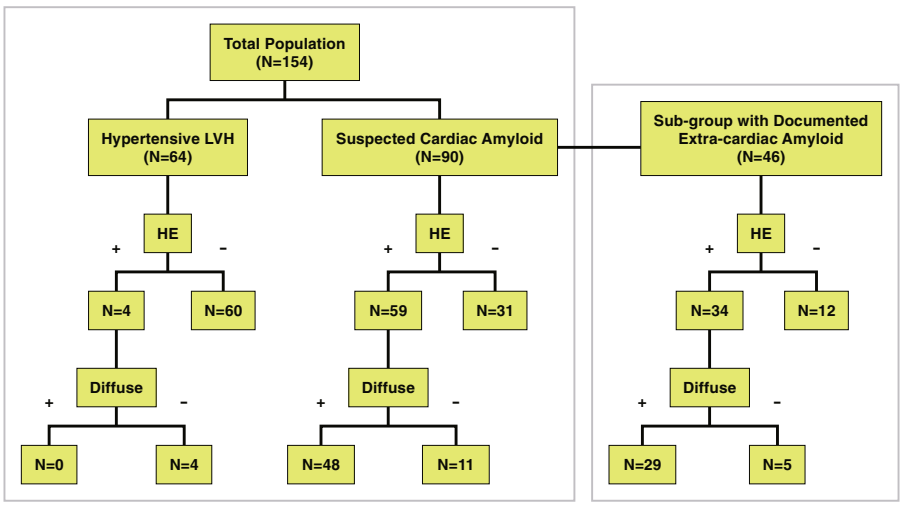

Figure 2. Diagram Showing the Prevalence of any HE and "Diffuse" Global HE Among Patients With Hypertensive LVH and Suspected Cardiac Amyloidosis

Findings in the subgroup with documented extracardiac amyloidosis are also shown. HE = hyperenhancement; LVH = left ventricular hypertrophy.

predictor in submodel 2 (HR: 6.2, 95% CI: 3.1 to 12.3; $p < 0.0001$). Again, the 2 submodels had similar overall predictive capability, with chi-square values of 103.1 and 101.6, respectively.

PATIENTS WITH SUSPECTED CA. Survival analyses were repeated with the removal of patients with hypertensive LVH. Results were similar to that for the whole population. For the primary endpoint, diffuse HE was the strongest predictor in submodel 1 (HR: 5.5, 95% CI: 2.7 to 11.0; $p < 0.0001$) and any HE the strongest predictor in submodel 2 (HR: 7.9, 95% CI: 3.1 to 20.1; $p < 0.0001$). For both submodels, the other independent predictors were serum creatinine and the presence of pleural effusion. For the secondary endpoint, diffuse HE (HR: 4.7, 95% CI: 2.4 to 9.4; $p < 0.0001$) or any HE (HR: 6.5, 95% CI: 2.6 to 16.0; $p < 0.0001$) was the strongest predictor in the multivariable models. Kaplan-Meier survival curves according to any or diffuse HE and primary or secondary endpoint are shown in Figure 4. Survival curves were adjusted for baseline differences in covariates (serum creatinine and presence of pleural effusion) found to independently predict outcome. In each case, the presence of HE (any or diffuse) was associated with a marked reduction in survival (all $p < 0.0001$). For instance, patients with diffuse HE had a 2-year survival rate of only 21% in comparison to 81% in those without HE. When survival analysis was performed after removal of patients with hereditary amyloidosis, there were no significant changes in the findings in that: 1) the same independent predictors were found for both submodels 1 and 2;

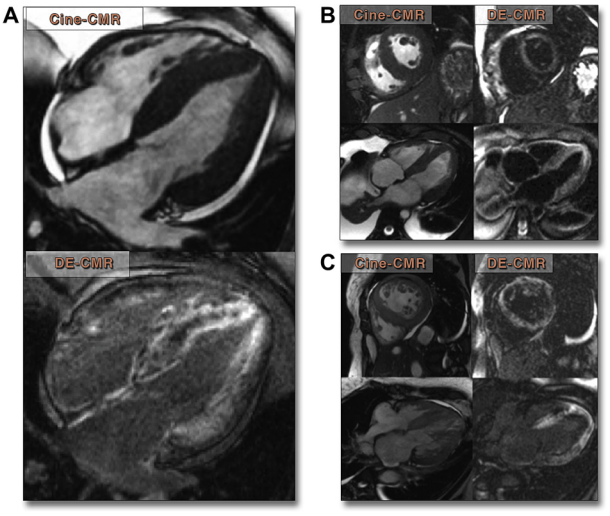

Figure 3. Typical Findings in 3 Patient Examples

(A) Four-chamber cine cardiac magnetic resonance (CMR) and delayed-enhancement cardiac magnetic resonance (DE-CMR) images in a 52-year-old man with systemic primary amyloidosis 5 months prior to his death. Diffuse, primarily subendocardial hyperenhancement is seen in both the left and right ventricles as well as in the interatrial septum. **(B)** A 61-year-old man with myeloma and new-onset heart failure showing diffuse subendocardial hyperenhancement. Patient died 6 months later. **(C)** A 49-year-old woman with restrictive cardiomyopathy by echocardiography and invasive hemodynamics showing diffuse hyperenhancement of the left ventricle. Patient died 45 days later.

Table 2. Predictors of Mortality in All Patients

	Univariable		Multivariable Model Using Diffuse HE		Multivariable Model Using Any HE	
	HR (95% CI)	p Value	HR (95% CI)	p Value	HR (95% CI)	p Value
All (n = 154)						
Clinical						
Age, yrs	1.03 (1.01–1.05)	0.02				
Male	0.8 (0.4–1.3)	0.32				
NYHA functional class	2.4 (1.8–3.1)	<0.0001	1.4 (1.0–1.9)	0.03	1.5 (1.1–2.0)	0.01
Right heart failure	5.4 (3.0–9.5)	<0.0001				
Dialysis	4.3 (2.2–6.9)	<0.0001				
Systolic blood pressure, mm Hg	0.97 (0.96–0.98)	<0.0001				
Diastolic blood pressure, mm Hg	0.96 (0.94–0.99)	0.0004				
Serum creatinine, mg/dl	1.3 (1.2–1.5)	<0.0001	1.3 (1.2–1.5)	<0.0001	1.3 (1.1–1.4)	0.0001
Elevated troponin-T	5.1 (2.6–10.2)	<0.0001				
Electrocardiography						
Low voltage	3.6 (2.0–6.6)	<0.0001				
Q wave	0.8 (0.4–1.4)	0.44				
Cine-CMR						
Mean LV wall thickness, mm	5.2 (2.6–10.6)	<0.0001				
LV mass index, g/m^2	1.02 (1.01–1.02)	<0.0001				
LV EDV index, ml/m^2	0.988 (0.975–1.002)	0.09				
LV ESV index, ml/m	1.009 (0.998–1.020)	0.11				
LV ejection fraction, %	0.97 (0.95–0.98)	<0.0001				
Pericardial effusion	2.5 (1.5–4.3)	0.0009				
Pleural effusion	4.9 (2.9–8.5)	<0.0001	2.6 (1.4–4.6)	0.002	3.1 (1.7–5.5)	0.0002
DE-CMR						
Any HE	12.8 (6.2–26.5)	<0.0001			6.5 (3.0–14.2)	<0.0001
Diffuse HE	12.0 (6.5–22.1)	<0.0001	6.0 (3.0–12.1)	<0.0001		
CAD-type HE	3.6 (1.8–7.2)	0.0003				
Focal non-CAD-type HE	0.6 (0.2–2.6)	0.52				
Model chi-square test			100.2	<0.0001	99.7	<0.0001

Continued on the next page

2) the HRs were nearly identical; and 3) diffuse HE (HR: 5.5, 95% CI: 2.6 to 11.4; $p < 0.0001$) or any HE (HR: 8.8, 95% CI: 3.1 to 24.9; $p < 0.0001$) were the most significant independent predictors of all-cause mortality.

In a separate multivariable modeling approach, only 4 variables were included to avoid the potential for overfitting. Three were pre-selected on the basis that they were well-known clinical markers of prognosis in cardiac amyloidosis—LV ejection fraction, ECG low-voltage pattern, and LV mass (23)—and the fourth was HE by CMR. With this approach (Table 3), diffuse HE was again the strongest predictor of mortality in submodel 1 (HR: 4.95, 95% CI: 2.12 to 11.6; $p = 0.0002$) and any HE was the strongest predictor in submodel 2 (HR: 9.25, 95% CI: 2.98 to 28.7; $p = 0.0001$).

PATIENTS WITH SYSTEMIC (EXTRACARDIAC) AMYLOIDOSIS. Among the subcohort of 46 patients that had documented systemic amyloidosis at the time of enrollment, 7 eventually underwent intravenous chemotherapy (melphalan) followed by stem cell transplantation and 5 received oral chemotherapy. There was no association between treatment regimen (stem cell transplantation, oral chemotherapy, or either treatment) and survival (all $p > 0.20$). Multivariable analysis demonstrated that diffuse HE (HR: 3.6, 95% CI: 1.4 to 9.5, $p = 0.009$) or any HE (HR: 6.1, 95% CI: 1.7 to 22.5, $p = 0.006$) were

Table 2. Continued

	Univariable		Multivariable Model Using Diffuse HE		Multivariable Model Using Any HE	
	HR (95% CI)	p Value	HR (95% CI)	p Value	HR (95% CI)	p Value
Echocardiography subgroup (n = 99)						
Echo parameters						
Mean LV wall thickness, mm	2.1 (0.9–5.3)	0.10				
E/A ratio	1.5 (1.2–1.8)	<0.0001				
Deceleration time, ms	0.94 (0.99–1.00)	0.05				
Deceleration time <160 ms	2.1 (1.1–3.7)	0.02				
E/E′ ratio	1.04 (1.01–1.07)	0.003				
E/E′ ratio >15	2.1 (0.9–4.7)	0.07				
Pseudonormal or restrictive diastology	1.6 (1.3–2.0)	<0.0001			1.4 (1.1–1.8)	0.004
Clinical						
Age, yrs	1.02 (1.00–1.05)	0.07				
Male	0.7 (0.4–1.2)	0.17				
NYHA functional class	2.0 (1.5–2.6)	<0.0001	1.4 (1.0–2.0)	0.04		
Right heart failure	3.5 (1.8–6.8)	0.0002				
Dialysis	3.3 (1.6–6.8)	0.001				
Systolic blood pressure, mm Hg	0.98 (0.96–0.99)	0.0005				
Diastolic blood pressure, mm Hg	0.97 (0.95–0.99)	0.006				
Serum creatinine, mg/dl	1.2 (1.1–1.4)	0.0003	1.3 (1.1–1.5)	0.0002	1.3 (1.1–1.5)	0.0002
Elevated troponin-T	3.6 (1.7–7.5)	0.0007				
Electrocardiography						
Low voltage	2.7 (1.4–5.2)	0.003				
Q wave	1.0 (0.5–1.8)	0.90				
Cine-CMR						
Mean LV wall thickness, mm	3.2 (1.5–6.9)	0.003				
LV mass index, g/m^2	1.01 (1.01–1.02)	0.004				
LV EDV index, ml/m^2	0.986 (0.971–1.000)	0.051				
LV ESV index, ml/m^2	1.002 (0.990–1.014)	0.79				
LV ejection fraction, %	0.98 (0.96–0.99)	0.008				
Pericardial effusion	1.9 (1.0–3.4)	0.04				
Pleural effusion	3.1 (1.7–5.7)	0.0002	2.0 (1.1–4.0)	0.04	2.5 (1.3–4.7)	0.008
DE-CMR						
Any HE	7.9 (3.5–17.9)	<0.0001			4.3 (1.8–10.3)	0.001
Diffuse HE	8.1 (4.1–16.0)	<0.0001	4.1 (1.8–9.2)	0.0007		
CAD-type HE	2.0 (0.9–4.4)	0.11				
Focal non-CAD-type HE	0.5 (0.1–2.1)	0.35				
Model chi-square test			58.4	<0.0001	56.8	<0.0001

CI = confidence interval; HR = hazard ratio; other abbreviations as in Table 1.

independent predictors of all-cause mortality. Patients with diffuse HE had a 2-year survival rate of only 23% in comparison with 75% in those without HE.

PATIENTS WITH ECHOCARDIOGRAPHY. Among the subcohort of 99 patients with echocardiography data, multivariable analysis showed nearly the same findings as in the whole population, suggesting that the echocardiography subcohort was representative of the entire group. For instance, in submodel 1, the same 4 variables (NYHA functional class, serum creatinine, presence of pleural effusion, and

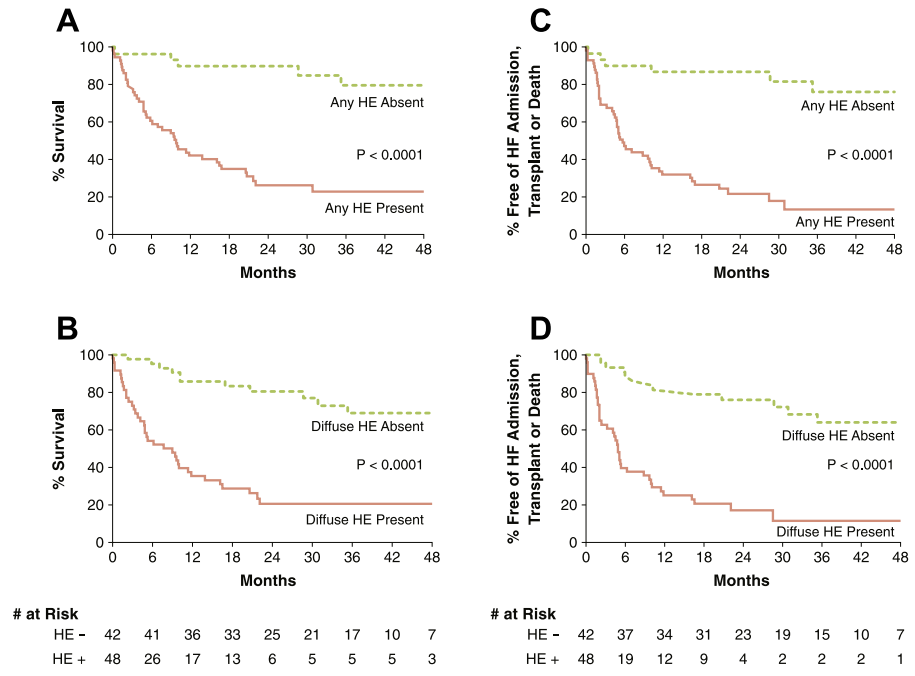

Figure 4. Kaplan-Meier Survival Curves for Patients With Suspected Cardiac Amyloidosis

The relationships between the presence of "any" or "diffuse" hyperenhancement (HE) and the primary endpoint of all-cause mortality are shown in **A** and **B**, respectively. The relationships between HE and the secondary endpoint of death, cardiac transplantation, or admission for heart failure (HF) are shown in **C** and **D**. The number at risk are shown for plots concerning diffuse HE. Survival curves were adjusted for baseline differences in covariates (serum creatinine and presence of pleural effusion) found to independently predict outcome. In all cases, the presence of HE was associated with significantly worse outcome.

diffuse HE) were found to be independent predictors of all-cause mortality in the echocardiography subcohort (Table 2, bottom) as in the entire population. Although univariable analysis revealed that several echocardiographic parameters were associated with all-cause mortality, only the presence of a pseudonormal or restrictive filling pattern was found to be an independent predictor, and only in submodel 2 incorporating "any HE" (Table 2).

Cardiac histopathology. During follow-up, myocardial tissue samples were obtained in 25 (28%) patients with suspected CA: 19 by EMB, 2 at time of cardiac transplantation, and 4 by post-mortem necropsy examination. Samples from 15 (60%) patients were positive for cardiac amyloid and demonstrated at least moderate interstitial amyloid protein deposition, frequently with perivascular infiltration. Varying degrees of myocyte loss and fibrosis were also observed, ranging from mild to severe. Of the 10 subjects found to be negative for cardiac amyloid, 5 demonstrated nonspecific patchy fibrosis, 1 revealed myocarditis, and 4 were normal.

All 15 patients with pathological evidence of CA demonstrated HE on DE-CMR. Of these, 14 (93%) had diffuse HE and 1 had focal subendocardial (CAD-type) HE. An example of the correlation between pathology and CMR is shown in Figure 5. Of the 10 patients without pathological evidence of CA, 7 had normal DE-CMR with no HE and 3 met criteria for diffuse HE. For all 3 latter patients, tissue samples were obtained by EMB, and DE-CMR demonstrated a relative sparing of HE along the right ventricular side of the interventricular septum, suggesting the potential for tissue sampling error. All 3 patients subsequently died but did not have autopsy performed. Overall, among the patients with myocardial histology, the sensitivity, specificity, and accuracy of diffuse HE in the diagnosis of CA was 93%, 70%, and 84%, respectively.

DISCUSSION

In this study, we tested the utility of a modified DE-CMR protocol to provide diagnostic and prognostic

Table 3. Multivariable Models With Pre-Selected Variables in Patients With Suspected Cardiac Amyloidosis

	Multivariable Model Using Diffuse HE		Multivariable Model Using Any HE	
Suspected CA (n = 90)	**HR (95% CI)**	**p Value**	**HR (95% CI)**	**p Value**
Non–DE-CMR variables				
LV ejection fraction, %	1.00 (0.98–1.02)	0.93	0.99 (0.98–1.01)	0.92
LV mass index, g/m^2	1.01 (0.99–1.01)	0.49	1.00 (0.99–1.00)	0.97
ECG low voltage	1.03 (0.51–2.08)	0.94	1.24 (0.64–2.40)	0.53
DE-CMR				
Any HE	—		9.25 (2.98–28.7)	0.0001
Diffuse HE	4.95 (2.12–11.6)	0.0002	—	
Model chi-square test	28.9	<0.0001	34.0	<0.0001

ECG = electrocardiogram; other abbreviations as in Table 1.

information in patients referred for suspected cardiac amyloidosis. Although several investigations have described a characteristic pattern on conventional DE-CMR—diffuse global subendocardial HE with variable epicardial extension (4–9)—it is commonly reported that imaging is difficult and that quality is often suboptimal (5–7,9,24). This is because conventional DE-CMR relies on correctly setting an imaging parameter (inversion time) to null signal from "normal" myocardium, yet normal myocardium may be absent in CA.

We used a T1 assessment sequence similar to that employed by Maceira et al. (5) But, rather than quantitatively calculating T1 offline in an effort to examine gadolinium kinetics, our goal was to prospectively test a practical approach to acquiring and interpreting the images in a "real-life" referral population. Our visual T1 assessment approach was

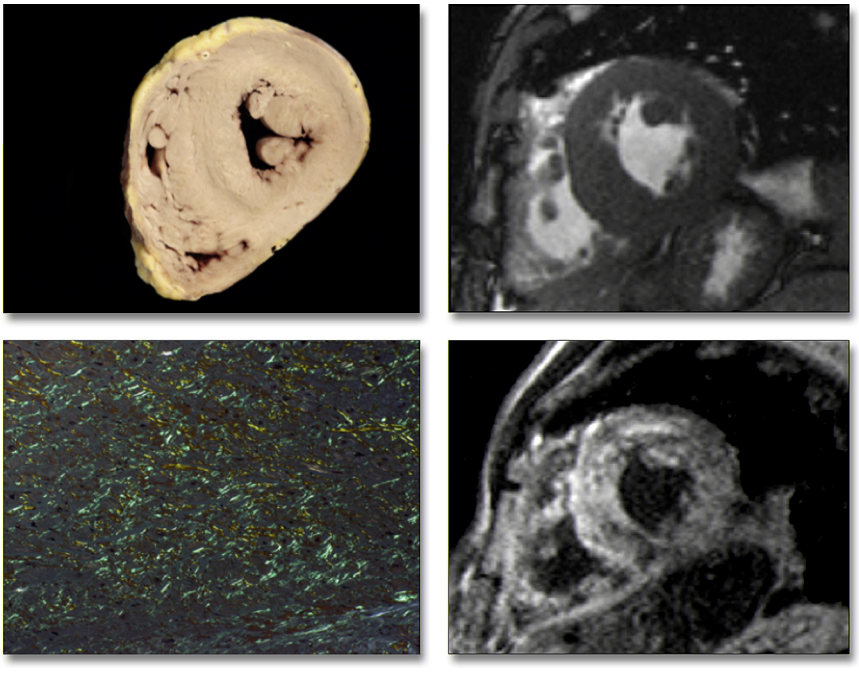

Figure 5. Pathology Correlation in a Patient With Primary Amyloidosis

Gross morphology **(top left)** shows globally-increased wall thickness of both the left and right ventricles, as also demonstrated in vivo by cine cardiac magnetic resonance **(top right)**. Tissue from the interventricular septum stained with Congo red shows marked interstitial amyloid deposition, with apple-green birefringence under polarized light **(bottom left)** correlating with diffuse hyperenhancement on delayed-enhancement cardiac magnetic resonance, which was particularly evident in the septum **(bottom right)**.

based on the concept that to first order, T1 is proportional to the inversion time needed to null signal ($T1 \approx [IT(null)]/\ln[2]$), and that following contrast administration, blood T1 is far shorter than that of normal myocardium (25). Thus, simply identifying that myocardial tissue reaches the null crossing (becomes black) at an earlier or the same inversion time as blood pool establishes that this tissue is abnormal (Fig. 1).

Although sophisticated evaluation of absolute T1 values are of growing interest (26), we suggest that a binary visual threshold approach, as validated in this study, provides certain advantages in the context of this disease state. The method is quick because the assessment is visual and performed without offline analysis; yet, it is objective because the threshold for dichotomizing normal from abnormal is unambiguous. Importantly, from a practical, hands-on perspective, the speed of the visual T1 assessment approach allows the findings to influence the scan itself by providing optimal settings for conventional DE-CMR, which immediately follows. For instance, if myocardium was globally abnormal on visual T1 assessment, then the inversion time for DE-CMR should be set to null blood pool rather than myocardium and images would accurately demonstrate global myocardial HE (Fig. 1, bottom, red frame), whereas if myocardium was erroneously nulled (Fig. 1, bottom, green frame), all regions may appear normal, highlighting the pitfalls of conventional DE-CMR without T1 assessment. The current study is the first to suggest that, in the presence of diffuse CA, the appropriate inversion time for conventional DE-CMR may be that needed to null the blood pool rather than myocardium.

With this approach, diffuse HE was observed in 48 of 90 patients with suspected CA, and among the subgroup with cardiac pathology validation ($n = 25$), the sensitivity and specificity of diffuse HE in the diagnosis of CA were 93% and 70%, respectively. Results were similar to that of earlier studies (4,7), although visual T1 assessment appeared to have higher sensitivity with lower specificity. For instance, Vogelsberg et al. (7), in an investigation of 33 patients referred for suspected CA, reported a sensitivity and specificity of 80% and 94%, respectively, for the detection of CA by DE-CMR in comparison with endomyocardial biopsy. Two issues should be considered, however, regarding the moderate specificity found in our study. First, unlike the report by Vogelsberg et al. (7), cardiac biopsy was not guided by the location of abnormalities on CMR and the LV free wall was not sampled. It is therefore possible that random biopsy of the right ventricular side of the interventricular septum (as in our study) may result in less accurate sampling of diseased myocardium and a higher "false-positive" rate for DE-CMR (27). This possibility is consistent with the finding that all 3 patients with diffuse HE and negative biopsy demonstrated relative sparing of HE along the right ventricular border of the interventricular septum. Second, it is notable that none of the 64 patients with hypertensive LVH had diffuse HE despite similar LV hypertrophy (mass) to patients with suspected CA. Thus, it appears that diffuse HE on visual T1 assessment is rare in cohorts with little to no risk of CA, and if patients with hypertensive LVH had been included in the analysis as true negatives, specificity would have increased to 96% (71 of 74), with sensitivity unchanged at 93%.

The principal finding in this cohort study was that the presence of diffuse HE by visual T1 assessment was a strong predictor of mortality, with an HR of 6.0 (95% CI: 3.0 to 12.1) on multivariable analysis. Three prior studies have aimed to evaluate the prognostic role of DE-CMR in patients with known or suspected CA and have reported conflicting results. The first, by Maceira et al. (10), followed 29 patients with known CA over a period of approximately 21 months. Given the small number of patients, multivariable analysis was not performed, and the presence of diffuse DE seen in 20 patients (69%) was not predictive of death. A post-hoc analysis of gadolinium kinetics, however, suggested that reduced differences in intramyocardial T1 (epicardial versus endocardial T1 at 2 min after contrast administration) was associated with increased mortality. Ruberg et al. (8), reported on 28 patients with systemic, light-chain amyloidosis in whom cardiac involvement was suspected. Although the presence of HE did not predict survival, there were only 5 deaths over a median follow-up period of 29 months. Austin et al. (4), retrospectively reviewed 47 patients with systemic amyloidosis and suspected CA or suspected restrictive cardiomyopathy who had undergone clinical CMR. In that study, the presence of diffuse HE by DE-CMR was predictive of prognosis; indeed, of multiple clinical characteristics including detailed noninvasive testing, diffuse HE was the sole predictive variable. However, events were few, with only 9 deaths during the 1-year follow-up period. In comparison to these earlier investigations, our study was substantially larger, and during a median follow-up period of approximately 2.5 years there were 54 deaths—far more than the 31 deaths in the 3 earlier studies combined.

Given that the value of any prognostic marker may change depending on the cohort studied, we performed multivariable analyses not only in the population as a whole, but also in several subgroups. The presence of diffuse HE was a strong independent predictor of mortality in: 1) the entire population (patients with suspected CA or hypertensive LVH, n = 154); 2) patients with echocardiography data (n = 99); 3) patients with suspected CA (n = 90); and 4) patients with documented systemic amyloidosis at the time of enrollment (n = 46). The HRs were similar among the 4 cohorts, indicating that diffuse HE identified by visual T1 assessment is a robust marker of outcome and suggesting its prognostic utility in a variety of referral populations. Additionally, it appears that the finding of focal, nondiffuse HE should not be disregarded, because the presence of "any HE" was also a strong independent predictor of mortality in the same 4 cohorts.

Study limitations. In an effort to keep the scan protocol short and clinically relevant, visual T1 assessment was performed using only 2 views (midventricular short-axis and 4-chamber long-axis planes). Additionally, the purpose of visual T1 assessment was to detect diffuse, global HE rather than all regions with focal HE; nonetheless, it is possible that additional views, such as a complete short-axis stack of images, could result in improved sensitivity for detecting CA compared with that found in the current study. We did not examine gadolinium kinetics, which may provide insight into the mechanism of diffuse HE in cardiac amyloidosis. However, as mentioned earlier, the primary goal of our study was to prospectively test a practical visual approach to performing and interpreting DE-CMR in the setting of diffuse, global myocardial disease. Only 1 dose of contrast (0.15 mmol/kg) with a clinically-convenient time window for T1 assessment (i.e., 5 to 10 min after contrast) was investigated. There should be caution in applying this method at different contrast doses and/or time windows. Our study was not designed to provide a systematic comparison with other biomarkers and imaging techniques known to have prognostic value in cardiac amyloidosis, such as B-type natriuretic peptide and strain Doppler imaging (21,28–30). Although a recent study reported superiority of DE-CMR compared with a battery of noninvasive tests commonly performed in patients with suspected CA (4), additional studies are clearly necessary to determine the clinical role of DE-CMR with or without visual T1 assessment in patients with suspected CA. The number of patients receiving pathological evaluation of the myocardium was relatively modest and therefore limits the evaluation of diagnostic accuracy for visual T1 assessment. A larger study with focus on histopathological validation is therefore desirable. Some patients were enrolled prior to Food and Drug Association warnings of nephrogenic systemic fibrosis in patients with severe renal insufficiency (glomerular filtration rate <30 ml/min/1.73 m^2) (11). None of the study participants were diagnosed with nephrogenic systemic fibrosis during follow-up; however, the use of DE-CMR will be limited in patients with significant renal impairment.

CONCLUSIONS

A modified DE-CMR protocol with visual T1 assessment was tested and shown to accurately identify patients with myocardial amyloid tissue deposition and those at a markedly increased risk of death. Overall, this suggests strong diagnostic and prognostic utility for the proposed DE-CMR protocol in patients referred for suspected cardiac amyloidosis.

Acknowledgment

The authors thank Selam Mequanint for assisting with the statistical analysis.

Reprint requests and correspondence: Dr. Raymond J. Kim, Duke Cardiovascular Magnetic Resonance Center, DUMC 3934, Durham, North Carolina 27710. *E-mail: raymond.kim@duke.edu.*

REFERENCES

1. Kyle RA, Greipp PR, O'Fallon WM. Primary systemic amyloidosis: multivariate analysis for prognostic factors in 168 cases. Blood 1986;68:220–4.
2. Cooper LT, Baughman KL, Feldman AM, et al. The role of endomyocardial biopsy in the management of cardiovascular disease: a scientific statement from the American Heart Association, the American College of Cardiology, and the European Society of Cardiology. J Am Coll Cardiol 2007;50:1914–31.
3. Kwong RY, Falk RH. Cardiovascular magnetic resonance in cardiac amyloidosis. Circulation 2005;111:122–4.
4. Austin BA, Tang WH, Rodriguez ER, et al. Delayed hyper-enhancement magnetic resonance imaging provides incremental diagnostic and prognostic utility in suspected cardiac amyloidosis. J Am Coll Cardiol Img 2009;2:1369–77.
5. Maceira AM, Joshi J, Prasad SK, et al. Cardiovascular magnetic resonance in cardiac amyloidosis. Circulation 2005;111:186–93.
6. van den Driesen RI, Slaughter RE, Strugnell WE. MR findings in cardiac

amyloidosis. AJR Am J Roentgenol 2006;186:1682–5.

7. Vogelsberg H, Mahrholdt H, Deluigi CC, et al. Cardiovascular magnetic resonance in clinically suspected cardiac amyloidosis: noninvasive imaging compared to endomyocardial biopsy. J Am Coll Cardiol 2008;51:1022–30.
8. Ruberg FL, Appelbaum E, Davidoff R, et al. Diagnostic and prognostic utility of cardiovascular magnetic resonance imaging in light-chain cardiac amyloidosis. Am J Cardiol 2009;103:544–9.
9. Syed IS, Glockner JF, Feng D, et al. Role of cardiac magnetic resonance imaging in the detection of cardiac amyloidosis. J Am Coll Cardiol Img 2010;3:155–64.
10. Maceira AM, Prasad SK, Hawkins PN, Roughton M, Pennell DJ. Cardiovascular magnetic resonance and prognosis in cardiac amyloidosis. J Cardiovasc Magn Reson 2008;10:54.
11. U.S. Food and Drug Administration. Information for healthcare professionals: gadolinium-based contrast agents for magnetic resonance imaging (marketed as magnevist, multihance, omniscan, optimark, prohance). Available at: http://www.fda.gov/Drugs/DrugSafety/PostmarketDrugSafetyInformationforPatientsandProviders/ucm142884.htm. Accessed December 5, 2010.
12. Chung YC, Lee VS, Laub G, Simonetti OP. Inversion recovery cine TrueFisp for optimizing TI in myocardial infarct imaging. Proc Int Soc Magn Reson Med 2002;10:219.
13. Huber A, Schoenberg SO, Spannagl B, et al. Single-shot inversion recovery TrueFisp for assessment of myocardial infarction. AJR Am J Roentgenol 2006;186:627–33.
14. Kim RJ, Wu E, Rafael A, et al. The use of contrast-enhanced magnetic resonance imaging to identify reversible myocardial dysfunction. N Engl J Med 2000;343:1445–53.
15. Kim RJ, Shah DJ, Judd RM. How we perform delayed enhancement imaging. J Cardiovasc Magn Reson 2003;5:505–14.
16. Mahrholdt H, Wagner A, Judd RM, Sechtem U, Kim RJ. Delayed enhancement cardiovascular magnetic resonance assessment of non-ischaemic cardiomyopathies. Eur Heart J 2005;26:1461–74.
17. Rahman JE, Helou EF, Gelzer-Bell R, et al. Noninvasive diagnosis of biopsy-proven cardiac amyloidosis. J Am Coll Cardiol 2004;43:410–5.
18. Prineas RJ, Crow RS, Blackburn HW. The minnesota code manual of electrocardiographic findings: standards and procedures for measurement and classification. Boston, MA: John Wright-PSG, 1982.
19. Nagueh SF, Appleton CP, Gillebert TC, et al. Recommendations for the evaluation of left ventricular diastolic function by echocardiography. Eur J Echocardiogr 2009;10:165–93.
20. Lauer MS, Blackstone EH, Young JB, Topol EJ. Cause of death in clinical research: time for a reassessment? J Am Coll Cardiol 1999;34:618–20.
21. Falk RH. Diagnosis and management of the cardiac amyloidoses. Circulation 2005;112:2047–60.
22. Kholova I, Niessen HW. Amyloid in the cardiovascular system: a review. J Clin Pathol 2005;58:125–33.
23. Kristen AV, Perz JB, Schonland SO, et al. Non-invasive predictors of survival in cardiac anyloidosis. Eur J Heart Fail 2007;9:617–24.
24. Perugini E, Rapezzi C, Piva T, et al. Non-invasive evaluation of the myocardial substrate of cardiac amyloidosis by gadolinium cardiac magnetic resonance. Heart 2006;92:343–9.
25. Schlosser T, Hunold P, Herborn CU, et al. Myocardial infarct: depiction with contrast-enhanced MR imaging—comparison of gadopentetate and gadobenate. Radiology 2005;236:1041–6.
26. Kellman P, Wilson JR, Xue H, et al. Extracellular volume fraction mapping in the myocardium, part 2: initial clinical experience. J Cardiovasc Magn Reson 2012;14:64.
27. Thomson LE. Cardiovascular magnetic resonance in clinically suspected cardiac amyloidosis: diagnostic value of a typical pattern of late gadolinium enhancement. J Am Coll Cardiol 2008;51:1031–2.
28. Bellavia D, Pellikka PA, Al-Zahrani GB, et al. Independent predictors of survival in primary systemic (Al) amyloidosis, including cardiac biomarkers and left ventricular strain imaging: an observational cohort study. J Am Soc Echocardiogr 2010;23:643–52.
29. Koyama J, Falk RH. Prognostic significance of strain Doppler imaging in light-chain amyloidosis. J Am Coll Cardiol Img 2010;3:333–42.
30. Tei C, Dujardin KS, Hodge DO, Kyle RA, Tajik AJ, Seward JB. Doppler index combining systolic and diastolic myocardial performance: clinical value in cardiac amyloidosis. J Am Coll Cardiol 1996;28:658–64.

Key Words: amyloid ■ magnetic resonance imaging ■ delayed enhancement.